RSC Advances

PAPER

View Article Online
View Journal | View Issue

Cite this: *RSC Adv.*, 2024, **14**, 12449

Tunable thermal diffusivity of silk protein assemblies based on their structural control and photo-induced chemical cross-linking†

Michihiro Tanaka,[a] Toshiki Sawada, *[a] Keiji Numata[bc] and Takeshi Serizawa *[a]

Received 22nd September 2023
Accepted 31st March 2024

DOI: 10.1039/d3ra06473e

rsc.li/rsc-advances

Silk, which has excellent mechanical properties and is lightweight, serves as a structural material in natural systems. However, the structural and functional applications of silk in artificial systems have been limited due to the difficulty in controlling its properties. In this study, we demonstrate the tunable thermal diffusivity of silk-based assemblies (films) based on secondary structural control and subsequent cross-linking. We found that the thermal diffusivity of the silk film is increased by the formation of β-sheet structures and dityrosine between Tyr residues adjacent to the β-sheet structures. Our results demonstrate the applicability of silk proteins as material components for thermally conductive biopolymer-based materials.

Introduction

Control over molecular self-assembly and resultant structures for materials application is an important goal for nanoarchitechtonics.[1–3] Bio(macro)molecules such as proteins (or peptides), nucleic acids, and saccharides have been considered as excellent components as the self-assembling nanomaterials.[4,5] Owing to their excellent mechanical properties, biodegradability, and biocompatibility, natural silk fibrous materials produced by silkworms and spiders have attracted considerable attention over the past several decades.[6–9] Their unique properties have enabled their application in various biomedical materials.[10–12] In particular, silk fibroin (SF), a natural protein obtained from silkworm cocoons (*Bombyx mori* (*B. mori*)) can be used as a cost-effective raw material for various material forms, such as films, sponges, and hydrogels, based on their structural controllability and processability.[13] Additionally, changing the secondary structure of SF from amorphous to antiparallel β-sheets using organic solvents (*i.e.*, methanol and ethanol)[14,15] or *via* water-vapor annealing[16] has been reported to result in the formation of an anti-parallel β-sheet structure, which enables further control over its characteristics. For example, the repetitive Gly Ala–Gly Ala–Gly Xaa peptide unit (Xaa: Ser, Tyr, or Ala), one of the main components of SF, provides stable structures because of the aforementioned β-sheet formation, resulting in unique mechanical, thermal, optical, and dielectric properties superior to those of traditional fibrous materials.[17,18] Recently, SF-based materials have become even more attractive as thermally conductive materials due to the potentially excellent thermal properties of structurally controlled SF, although silk-based textiles have been used as thermal insulators for thousands of years.[19,20]

With advances in electronic devices, heat management has become a significant problem. Traditionally, the utilization of metal or inorganic heat sinks has been effective for such devices and thermal interface materials, which serve as heat transfer media between the heat source and sink, have been essential to guarantee reliable heat dissipation from the devices. Furthermore, recent considerable interest in thin and flexible electronic devices requires the development of flexible thermally conductive materials for stable electronic paper and wearable devices. Organic polymers, which generally have soft and moldable properties, are promising as flexible thermally conductive materials; however, the low thermal conductivity of bulk polymer films renders them inferior to metals and ceramics in material applications where effective thermal management is required.[21,22] The development of polymeric materials with high thermal conductivity remains a challenge. Recent studies have revealed that bulk films comprising structurally regular biopolymers, such as nanocellulose, filamentous viruses, and designed tandem-repeat proteins, are promising thermally conductive materials.[19,20,23–30]

The chemical cross-linking of SF materials has recently been used in addition to physical cross-linking, through the formation of crystalline antiparallel β-sheets, to improve and/or pioneer physicochemical properties and functions. With relatively high amounts of Tyr residues in SF (Tyr: 5.3 mol% Gly:

[a]*Department of Chemical Science and Engineering, School of Materials and Chemical Technology, Tokyo Institute of Technology, 2-12-1 Ookayama, Meguro-ku, Tokyo 152-8550, Japan. E-mail: sawada@mac.titech.ac.jp; serizawa@mac.titech.ac.jp*

[b]*Department of Material Chemistry, Graduate School of Engineering, Kyoto University, Kyoto-Daigaku-Katsura, Nishikyo-ku, Kyoto 615-8510, Japan*

[c]*Biomacromolecules Research Team, RIKEN Center for Sustainable Resource Science, 2-1 Hirosawa, Wako-shi, Saitama 351-0198, Japan*

† Electronic supplementary information (ESI) available. See DOI: https://doi.org/10.1039/d3ra06473e

45.9 mol%, Ala: 30.3 mol%, Ser: 12.1 mol%, and Val: 1.8 mol%),[31,32] it was reported that the oxidation of adjacent Tyr residues by horseradish peroxidase or ultraviolet (UV) light irradiation resulted in chemically cross-linked SF by the effective formation of dityrosine.[33] Such a structural control strategy involving the formation of specific secondary structures and chemical cross-linking would be useful for designing and realizing SF-based materials with improved properties and functions. Herein, we demonstrate the high thermal diffusivity of assemblies (films) comprising SF with controlled secondary and cross-linked structures (Fig. 1A). Immersing SF films in water/methanol mixed solvents resulted in the formation of β-sheet structures. Fluorescence measurements revealed the formation of dityrosine upon UV irradiation of the films. Thermal diffusivity measurements by temperature wave analysis[34] demonstrated the tunable thermal diffusivity of the SF films using a structural control strategy. Our results are expected to be useful for the design of wearable electronic devices that combine excellent heat dissipation performance with the original biocompatibility and mechanical strength of SF.

Results and discussion

B. mori silkworm-based SF films were prepared according to a previously reported method.[13] In brief, *B. mori* silkworm silk fibers were first degummed and further dissolved in an LiBr solution. The solution was purified and concentrated by reverse dialysis against an aqueous solution. The resultant SF solution was cast on a plastic Petri dish, and SF films with several tens of micrometers thick were obtained (Fig. 1B).

It has been reported that, during the evaporation of a colloidal solution in the preparation of cast films, the deposition process of the solute varies with the position of the resultant film. This is due to differences in evaporation kinetics based on the convection of the solute,[35,36] resulting in different heat conduction performances. Thus, we first characterized assembled structures and thermal diffusivity at different positions of the SF film. Polarized optical microscopy (POM) was performed to characterize the ordered structures of SF in the films (Fig. 2A and S1†). The images show little birefringence, indicating that non-oriented structures were formed at all positions of the film. Attenuated total reflection Fourier transform infrared (ATR/FT-IR) spectra reveal a sharp band at

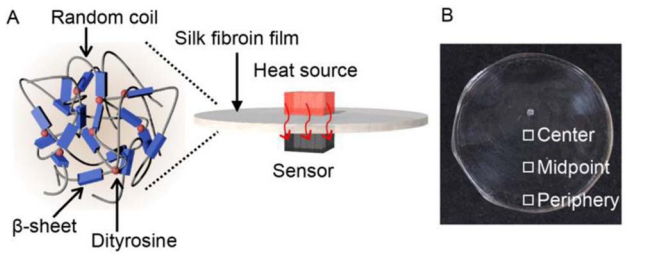

Fig. 1 (A) Schematic and (B) photograph of silk fibroin (SF) films with controlled secondary (β-sheet) and cross-linking (dityrosine) structures for excellent thermally conductive properties.

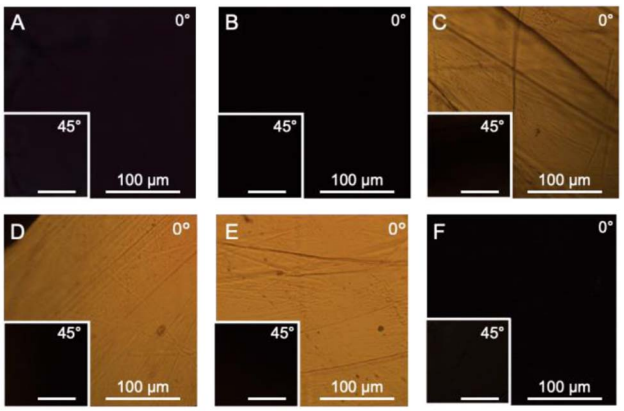

Fig. 2 Polarized optical microscopy (POM) observation of SF films with various structures: (A) original (periphery), (B) immersed, (C) stretched (10%), (D) stretched (20%), (E) stretched (30%), and (F) irradiated SF films.

approximately 1640 cm^{-1}, which is primarily assigned to the random coil structures of C═O stretching (Amide I) (Fig. 3A and S2†),[37] indicating that they constituted the entire film. In contrast, the thermal diffusivity values of the SF film at the periphery, the midpoint (between the periphery and center), and the center (Fig. 1B) in a perpendicular direction were measured by temperature wave analysis (Fig. 4 and S3†), and the thermal diffusivity values at the periphery (7.6×10^{-8} m^2 s^{-1}) were slightly greater than those at the other positions, showing slightly different heat conduction at the different film positions. The results suggest that the molecular and/or assembled structures of SF differed with the position of the films. In fact,

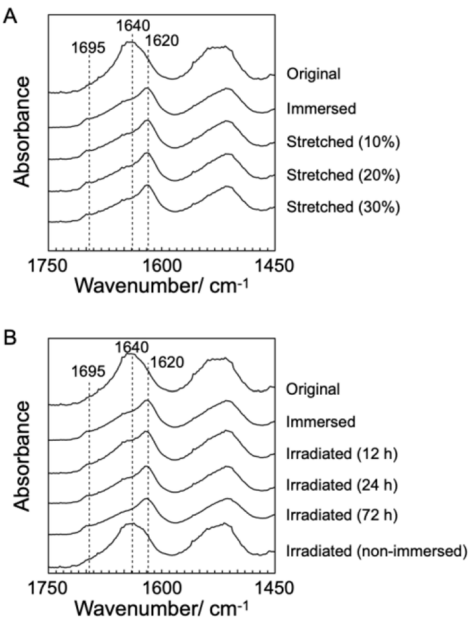

Fig. 3 Attenuated total reflection Fourier transform infrared (ATR/FT-IR) spectroscopy of the SF films with various structures. Effects of (A) immersing and stretching and (B) immersing and UV irradiation on the thermal secondary structures of the SF films.

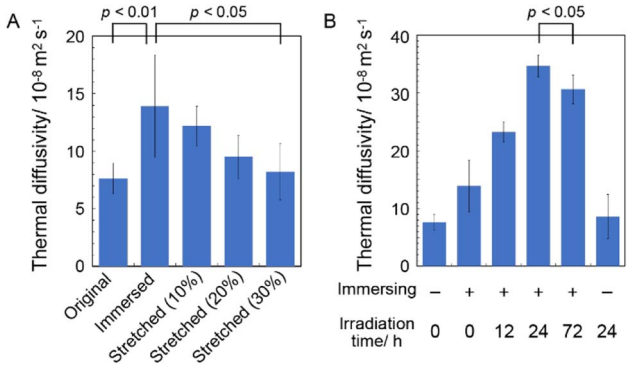

Fig. 4 Comparison of the thermal diffusivity values of the original, immersed, and irradiated SF films. Effects of (A) immersing and stretching and (B) immersing and UV irradiation on the thermal diffusivity values of the SF films. All the values were obtained at the periphery.

differential transformer methods revealed that the film thicknesses at the periphery, midpoint, and center were 93.6 ± 6.0, 55.8 ± 3.3, and 45.2 ± 3.3 μm, respectively. Therefore, the periphery of the SF films may be formed *via* convection in the solution, where it can condense more effectively than at the other positions. Thus, we focused on the periphery position in further experiments.

To characterize SF structures and determine their thermal diffusivities, the assembled SF structures were immersed in a mixed solution of methanol and water to control secondary structures. The immersed film was further stretched to form oriented structures with different elongation ratios (10%, 20%, and 30%). In another approach, the original and immersed SF films were irradiated with UV light to cross-link the Tyr residues. POM was performed on the films (Fig. 2B–F). Similar to the original film, the immersed film showed no birefringence, indicating that the immersion process had little effect on the SF-oriented structures. In contrast, uniform birefringence was observed in the immersed- and subsequently stretched-film, which was darkened by 45° rotation of the film, suggesting that the structures comprise oriented structures as nematic liquid crystals. Birefringence increased with increasing elongation ratio, as observed in POM images, demonstrating the effects of the stretching procedure on the oriented structures of the SF films. The IR spectra of the stretched films showed two bands, corresponding to parallel (approximately 1620 cm^{-1}) and antiparallel β-sheet structures (approximately 1695 cm^{-1}) in the Amide I region (Fig. 3A), indicating that SF in the original film underwent a structural transition from a random coil to a β-sheet during the immersion process. A slight change in the bands in the Amide I region was observed with the elongation ratio, suggesting that the molecular chains of SF were oriented in the direction of stretching, although the β-sheet structure formed by the immersion process was maintained.

Furthermore, the POM images of film subjected to immersion and UV irradiation did not show birefringence, demonstrating non-oriented states similar to the original one. POM observations demonstrated that the stretching process produced oriented SF structures, whereas UV irradiation did not. The IR spectra of irradiated films were similar to those of immersed films (Fig. 3B), suggesting that UV irradiation did not affect the secondary structures of the SF films.

Absorption spectra of the SF films were measured (Fig. S4†) to characterize the effect of irradiation. After irradiation, the optical density around 310 nm increased in a time-dependent manner from 12 to 72 h, indicating a photo-induced increase in cross-linking of tyrosine and/or oxidization of aromatic amino acids.[38,39] The fact that the absorption spectrum after 72 h does not show a dramatic increase in baselines indicates that the possible oxidation has not led to sufficient degradation to decrease the transparency of the film and is a minor effect. Fluorescence spectroscopy measurements of SF resolubilized with 1,1,1,3,3,3-hexafluoro-2-propanol were performed to determine the formation of dityrosine in the SF films. Cross-linked tyrosine shows a fluorescence peak at approximately 400 nm upon excitation at 275 nm (Fig. S5†). Peaks corresponding to the excitation light are observed in the characterization of the original and immersed SF films. After UV irradiation for 24 and 72 h, shoulder peaks at approximately 400 nm are observed, although no additional peaks are observed after 12 h. The results indicated the formation of the cross-linked structure of dityrosine during irradiation, although SF was assembled in film states. Combining these spectroscopic measurements, it was shown that the cross-linked structure of dityrosine increased with increasing irradiation time, although aromatic amino acids were hardly oxidized.

The thermal diffusivity values of the immersed, stretched, and irradiated SF films in the perpendicular direction were measured using temperature wave analysis (Fig. 4). The thermal diffusivity of the immersed film (14×10^{-8} m^2 s^{-1}) was higher than that of the original film, demonstrating the excellent heat (in this case, phonon) conduction capability of the immersed film, which is consistent with the crystalline β-sheet-structured SF, possibly due to the crystallization of SF chains *via* β-sheet formation. Because correctly formed β-sheet structures reportedly have superior anisotropic phonon conduction compared to that of other secondary structures,[40,41] they are believed to effectively conduct phonons between the SF chains. Furthermore, the thermal diffusivity of the stretched film decreased with increasing elongation ratio, suggesting that the orientation of the SF chains along the plane decreased their thermal diffusivity in the perpendicular direction. Stretching of silk fibers can greatly enhance the thermal conductivity against the fiber axis because of suitably oriented β-sheet structures;[42] thus, it was suggested that thermal diffusivity in the perpendicular direction (*i.e.*, between the SF chains) of the film decreased with the stretching procedure, possibly due to the unpreferred orientation of the β-sheet structures in the measurement direction.

The effect of the cross-linking of SF in the film on its thermal diffusivity was determined. When the SF film was irradiated with UV light after the immersion procedure, thermal diffusivity increased with increasing irradiation time (up to 24 h). After 72 h, the value was the same as that at 24 h, within experimental error. The results showed a similar trend to the increase in

dityrosine observed in absorption and fluorescence measurements. The thermal diffusivity value after irradiation for 24 h was 34 $\times$ 10^{-8} m^2 s^{-1}, indicating that the cross-linking of tyrosine residues (*i.e.*, dityrosine formation) affected the increase in thermal diffusivity. Furthermore, a greater amount of dityrosine after irradiation for 72 h was observed in fluorescence spectra than after 24 h; thus, longer irradiation than 24 h, which did not significantly affect thermal diffusivity, was required, possibly due to sufficient dityrosine formation with 24 h of irradiation to effectively conduct phonons in SF assemblies. Because the secondary and oriented structures of SF were unchanged during irradiation, newly prepared covalent bonds were speculated to have efficiently contributed to the increased thermal diffusivity. In fact, the cross-sectional scanning electron microscopy (SEM) profiles of the original, immersed, and irradiated (72 h) films reveal unchanged nanostructures (Fig. 5A–C). Additionally, the immersion procedure affected the surface morphology, whereas UV irradiation did not (Fig. 5D–F), proving the importance of cross-linking. Importantly, when the original film was irradiated with UV light without an immersion procedure, the thermal diffusivity was the same as that of the original film within experimental error. The results demonstrated the essential role of β-sheet formation by immersion in achieving high thermal diffusivity by photo-irradiation. Because changes in secondary, oriented, and macroscopic structures were not shown during irradiation, cross-linking of Tyr residues observed by absorbance and fluorescence measurements would affect the improved thermal diffusivity (that is, phonon conduction) of the SF films formed with the β-sheet structures. The repetitive hexapeptide partially containing the Tyr residue unit in SF was important for β-sheet formation; therefore, the cross-linking of Tyr residues adjacent to the β-sheet structures possibly enhanced phonon conduction. Together, these observations demonstrate that the cross-linking of Tyr residues (*i.e.*, dityrosine formation) in the β-sheet-structured SF plays an important role in efficient phonon transport for achieving SF materials with high thermal diffusivity.

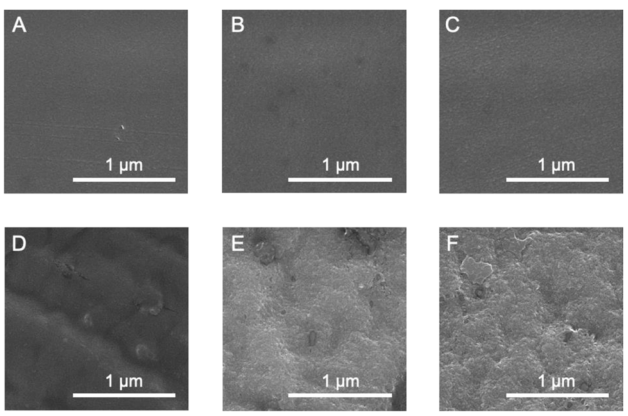

Fig. 5 Scanning electron microscopy images of (A–C) cross-sections and (D–F) surfaces of (A and D) original; (B and E) immersed; and (C and F) irradiated (24 h) films.

Conclusions

In this study, we investigated the thermal diffusivity of solid films comprising SF, prepared under various conditions. POM and IR measurements showed the successful preparation of various secondary and cross-linked structured films by immersion of appropriate solvents and subsequent UV irradiation. The immersion procedure, which resulted in a structural transition of SF from a random coil to a β-sheet, caused a slight increase in the thermal diffusivity, possibly by enabling suitable phonon transport. With increasing irradiation time, the UV light irradiation of the immersed film increased the thermal diffusivity, demonstrating the role of the cross-linked structures *via* the formation of dityrosine. The thermal diffusivity of the SF films prepared under suitable conditions was approximately five times that of the original SF film, demonstrating the tunable ability for phonon transport in SF. This study clearly elucidates the potential applicability of SF to a novel class of thermally conductive materials comprising bioorganic polymers.

Author contributions

T. Sawada and T. Serizawa designed the project. T. Sawada and M. Tanaka conceived and designed the experiments and analyzed the data. M. Tanaka performed all experiments. K. Numata directed the preparation and structural control of silk fibroin films. M. Tanaka, T. Sawada, and T. Serizawa wrote the manuscript.

Conflicts of interest

There are no conflicts to declare.

Acknowledgements

The authors wish to thank the Open Facility Center, Materials Analysis Division (Tokyo Tech) for SEM observations. This work was supported by the Japan Science and Technology Agency (JST) through the Fusion Oriented Research for Disruptive Science and Technology Grant Number JPMJFR211P, Grant-in-Aid for Scientific Research (C) (21K05182) from the Japan Society for the Promotion of Science (JSPS), MEXT Program: Data Creation and Utilization-Type Material Research and Development Project Grant Number JPMXP1122714694, and Moritani Scholarship Foundation for T. Sawada, and supported by JST SPRING, Grant Number JPMJSP2106 for M. Tanaka.

Notes and references

1 Y. Y. Zhan and S. Hiraoka, *Bull. Chem. Soc. Jpn.*, 2021, **94**, 2329–2341.
2 D. L. Jiang, *Bull. Chem. Soc. Jpn.*, 2021, **94**, 1215–1231.
3 K. Ariga and M. Shionoya, *Bull. Chem. Soc. Jpn.*, 2021, **94**, 839–859.
4 H. Inaba and K. Matsuura, *Bull. Chem. Soc. Jpn.*, 2021, **94**, 2100–2112.

5 Y. Hata and T. Serizawa, *Bull. Chem. Soc. Jpn.*, 2021, **94**, 2279–2289.
6 C. C. Guo, C. M. Li and D. L. Kaplan, *Biomacromolecules*, 2020, **21**, 1678–1686.
7 E. M. Pritchard and D. L. Kaplan, *Expert Opin. Drug Delivery*, 2011, **8**, 797–811.
8 Z. Z. Shao and F. Vollrath, *Nature*, 2002, **418**, 741.
9 K. Numata, *Polym. J.*, 2020, **52**, 1043–1056.
10 T. B. Aigner, E. DeSimone and T. Scheibel, *Adv. Mater.*, 2018, **30**, 1704636.
11 C. Holland, K. Numata, J. Rnjak-Kovacina and F. P. Seib, *Adv. Healthcare Mater.*, 2019, **8**, 1800465.
12 G. Janani, M. Kumar, D. Chouhan, J. C. Moses, A. Gangrade, S. Bhattacharjee and B. B. Mandal, *ACS Appl. Bio Mater.*, 2019, **2**, 5460–5491.
13 D. N. Rockwood, R. C. Preda, T. Yucel, X. Q. Wang, M. L. Lovett and D. L. Kaplan, *Nat. Protoc.*, 2011, **6**, 1612–1631.
14 X. Chen, H. F. Cai, S. J. Ling, Z. Z. Shao and Y. F. Huang, *Appl. Spectrosc.*, 2012, **66**, 696–699.
15 S. Kaewpirom and S. Boonsang, *RSC Adv.*, 2020, **10**, 15913–15923.
16 X. Hu, K. Shmelev, L. Sun, E. S. Gil, S. H. Park, P. Cebe and D. L. Kaplan, *Biomacromolecules*, 2011, **12**, 1686–1696.
17 W. W. Huang, S. J. Ling, C. M. Li, F. G. Omenetto and D. L. Kaplan, *Chem. Soc. Rev.*, 2018, **47**, 6486–6504.
18 Z. T. Zhou, S. Q. Zhang, Y. T. Cao, B. Marelli, X. X. Xia and T. H. Tao, *Adv. Mater.*, 2018, **30**, 1706983.
19 K. Uetani, T. Okada and H. T. Oyama, *Biomacromolecules*, 2015, **16**, 2220–2227.
20 J. A. Diaz, Z. J. Ye, X. W. Wu, A. L. Moore, R. J. Moon, A. Martini, D. J. Boday and J. P. Youngblood, *Biomacromolecules*, 2014, **15**, 4096–4101.
21 Z. Wang, J. A. Carter, A. Lagutchev, Y. K. Koh, N.-H. H. Seong, D. G. Cahill and D. D. Dlott, *Science*, 2007, **317**, 787–790.
22 H. G. Chae and S. Kumar, *Science*, 2008, **319**, 908–909.
23 D. C. Hu, W. S. Ma, Z. L. Zhang, Y. Ding and L. Wu, *ACS Appl. Mater. Interfaces*, 2020, **12**, 11115–11125.
24 T. Sawada, Y. Murata, H. Marubayashi, S. Nojima, J. Morikawa and T. Serizawa, *Sci. Rep.*, 2018, **8**, 5412.
25 T. Sawada, Y. Murata, H. Marubayashi, S. Nojima, J. Morikawa and T. Serizawa, *Viruses*, 2018, **10**, 608.
26 T. Sawada, T. Tsuruoka, N. Ueda, H. Marubayashi, S. Nojima, J. Morikawa and T. Serizawa, *Polym. J.*, 2020, **52**, 803–811.
27 J. A. Tomko, A. Pena-Francesch, H. H. Jung, M. Tyagi, B. D. Allen, M. C. Demirel and P. E. Hopkins, *Nat. Nanotechnol.*, 2018, **13**, 959–964.
28 G. Wang, M. Kudo, K. Daicho, S. Harish, B. Xu, C. Shao, Y. Lee, Y. Liao, N. Matsushima, T. Kodama, F. Lundell, L. D. Söderberg, T. Saito and J. Shiomi, *Nano Lett.*, 2022, **22**, 8406–8412.
29 T. Tong, Y. Li, C. Wu, C. Ma, J. Yang and Z. Wei, *Int. J. Therm. Sci.*, 2023, **185**, 108057.
30 T. Yamato, T. Wang, W. Sugiura, O. Laprévote and T. Katagiri, *J. Phys. Chem. B*, 2022, **126**, 3029–3036.
31 M. Tsukada, G. Freddi, N. Minoura and G. Allara, *J. Appl. Polym. Sci.*, 1994, **54**, 507–514.
32 A. Nishida, M. Yamada, T. Kanazawa, Y. Takashima, K. Ouchi and H. Okada, *Chem. Pharm. Bull.*, 2010, **58**, 1480–1486.
33 N. Johari, L. Moroni and A. Samadikuchaksaraei, *Eur. Polym. J.*, 2020, **134**, 109842.
34 J. Morikawa and T. Hashimoto, *J. Appl. Phys.*, 2009, **105**, 113506.
35 R. D. Deegan, O. Bakajin, T. F. Dupont, G. Huber, S. R. Nagel and T. A. Witten, *Nature*, 2021, **592**, E12.
36 H. Hu and R. G. Larson, *J. Phys. Chem. B*, 2006, **110**, 7090–7094.
37 P. I. Haris and D. Chapman, *Biopolymers*, 1995, **37**, 251–263.
38 A. Sionkowska and A. Planecka, *Polym. Degrad. Stab.*, 2011, **96**, 523–528.
39 S. Lee, S. H. Kim, Y.-Y. Jo, W.-T. Ju, H.-B. Kim and H. Kweon, *Biomolecules*, 2021, **11**, 70.
40 L. Zhang, Z. T. Bai, H. Ban and L. Liu, *Phys. Chem. Chem. Phys.*, 2015, **17**, 29007–29013.
41 L. Zhang, T. L. Chen, H. Ban and L. Liu, *Nanoscale*, 2014, **6**, 7786–7791.
42 X. Huang, G. Liu and X. Wang, *Adv. Mater.*, 2012, **24**, 1482–1486.